Crystal Structures of a Mutant (βK87T) Tryptophan Synthase $\alpha_2\beta_2$ Complex with Ligands Bound to the Active Sites of the α- and β-Subunits Reveal Ligand-Induced Conformational Changes‡

Sangkee Rhee,[§,||] Kevin D. Parris,[§,||,⊥] C. Craig Hyde,[#] S. Ashraf Ahmed,[○] Edith Wilson Miles,[○] and David R. Davies*[,||]

Laboratory of Molecular Biology and Laboratory of Biochemistry and Genetics, National Institute of Diabetes and Digestive and Kidney Diseases, and Laboratory of Structural Biology, National Institute of Arthritis and Musculoskeletal and Skin Diseases, National Institutes of Health, Bethesda, Maryland 20892

Received January 8, 1997; Revised Manuscript Received April 11, 1997[⊗]

ABSTRACT: Three-dimensional structures are reported for a mutant (βK87T) tryptophan synthase $\alpha_2\beta_2$ complex with either the substrate L-serine (βK87T-Ser) or product L-tryptophan (βK87T-Trp) at the active site of the β-subunit, in which both amino acids form external aldimines with the coenzyme, pyridoxal phosphate. We also present structures with L-serine bound to the β site and either α-glycerol 3-phosphate (βK87T-Ser-GP) or indole-3-propanol phosphate (βK87T-Ser-IPP) bound to the active site of the α-subunit. The results further identify the substrate and product binding sites in each subunit and provide insight into conformational changes that occur upon formation of these complexes. The two structures having ligands at the active sites of both α- and β-subunits reveal an important new feature, the ordering of α-subunit loop 6 (residues 179−187). Closure of loop 6 isolates the active site of the α-subunit from solvent and results in interaction between αThr183 and the catalytic residue αAsp60. Other conformational differences between the wild type and these two mutant structures include a rigid-body rotation of the α-subunit of ∼5° relative to the β-subunit and large movements of part of the β-subunit (residues 93−189) toward the rest of the β-subunit. Much smaller differences are observed in the βK87T-Ser structure. Remarkably, binding of tryptophan to the β active site results in conformational changes very similar to those observed in the βK87T-Ser-GP and βK87T-Ser-IPP structures, with exception of the disordered α-subunit loop 6. These large-scale changes, the closure of loop 6, and the movements of a small number of side chains in the $\alpha-\beta$ interaction site provide a structural base for interpreting the allosteric properties of tryptophan synthase.

The control and coordination of chemical events in the living cell are often achieved by allosteric proteins (Perutz, 1989). Allosteric interactions occur when the binding of one ligand at a specific site is influenced by the binding of another ligand at a different (allosteric) site. An important problem in the elucidation of the allosteric mechanism is the structural basis for ligand-mediated communication between topologically distinct binding sites. An ideal system for investigating this problem is the bacterial tryptophan synthase $\alpha_2\beta_2$ complex (EC 4.2.1.20) that catalyzes the last two steps in the biosynthesis of L-tryptophan [for reviews see Miles (1979, 1986, 1991a, 1995), Miles et al. (1994), Swift and Stewart (1991), and Yanofsky and Crawford (1972)]. In the first step, IGP[1] is cleaved to G3P and indole at the active site of the α-subunit (α reaction). In the second reaction, indole reacts with L-serine in a PLP-dependent reaction at the active site of the β-subunit (β reaction). The overall reaction, which is formally the sum of the α and β reactions, is termed the $\alpha\beta$ reaction.

α reaction: IGP → indole + G3P

β reaction: L-serine + indole → L-tryptophan + H_2O

$\alpha\beta$ reaction: L-serine + IGP → L-tryptophan + G3P + H_2O

The initial 2.5 Å resolution crystal structure of the tryptophan synthase $\alpha_2\beta_2$ complex (Hyde et al., 1988) and the subsequent 1.9 Å resolution structure[2] revealed many structural features of the enzyme, including the binding site of the substrate analog IPP at the active site of the α-subunit, the location of the PLP coenzyme at the active site of the β-subunit, and the presence of a hydrophobic tunnel connecting the active sites of the α- and β-subunits. It was

‡ The coordinates of the structures have been deposited in the Brookhaven Protein Data Bank (PDB) under the names 1UBS for the βK87T-serine, 2TRS for the βK87T-serine-IPP, 2TSY for the βK87T-serine-GP, and 2TYS for the βK87T-tryptophan complex.

* Author to whom correspondence and reprint requests should be addressed: National Institutes of Health, Bldg 5, Rm 338, Bethesda, MD 20892. Tel: 301-496-4295. Fax: 301-496-0201.

§ The first two authors contributed equally to this work.

|| Laboratory of Molecular Biology.

⊥ Present address: Wyeth-Ayerst Research, CN8000, Princeton, NJ 08543.

Laboratory of Structural Biology.

○ Laboratory of Biochemistry and Genetics.

⊗ Abstract published in *Advance ACS Abstracts,* June 1, 1997.

[1] Abbreviations: IGP, indole-3-glycerol phosphate; G3P, glyceraldehyde 3-phosphate; PLP, pyridoxal 5′-phosphate; IPP, indole-3-propanol phosphate; GP, DL-α-glycerol 3-phosphate; PEG, poly(ethylene glycol); rms, root mean square.

[2] C. C. Hyde, K. D. Parris, T. N. Bhat, C. Brown, S. A. Ahmed, E. W. Miles, and D. R. Davies, in preparation.

S0006-2960(97)00042-1 CCC: $14.00

Scheme 1: Reactions at the Active Site of the β-Subunit in the (A) Wild-Type $\alpha_2\beta_2$ Complex and the (B) βK87T $\alpha_2\beta_2$ Complex

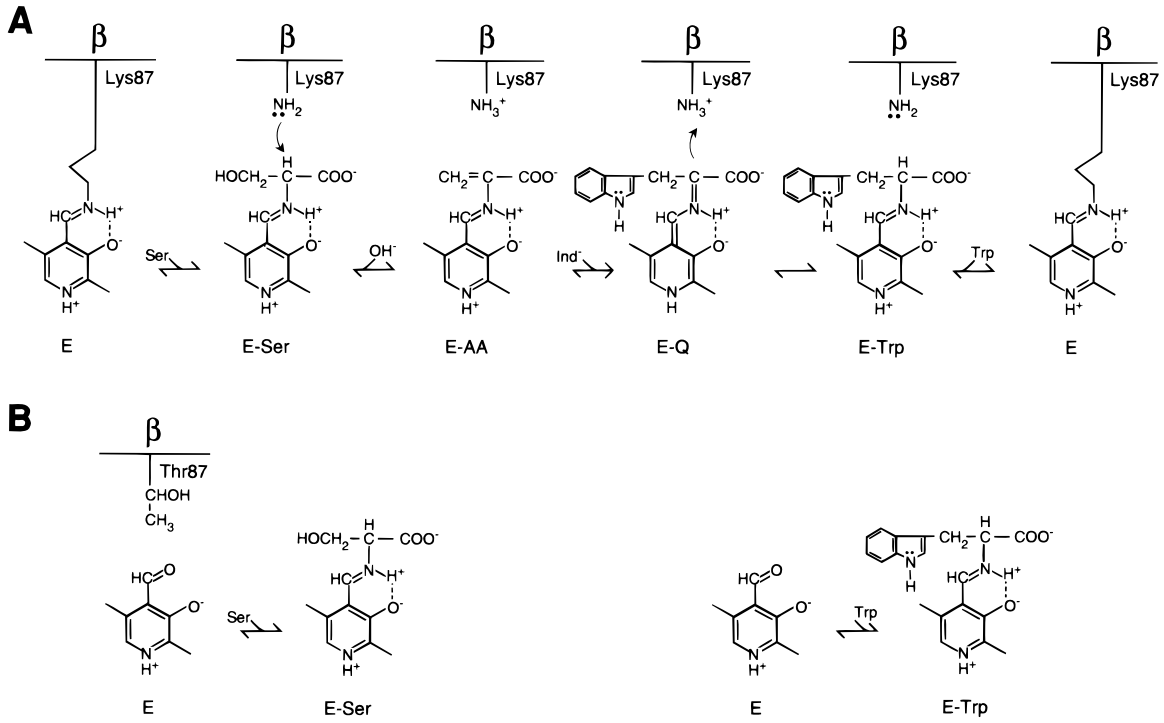

proposed that this tunnel permits indole, the product of the α-reaction, to diffuse to the active site of the β-subunit without being released into the solvent. Crystallographic studies of the wild-type $\alpha_2\beta_2$ complex showed that exchange of potassium or cesium for sodium ion altered the conformation of the tunnel by removing a side chain of βPhe280 that blocked the tunnel (Rhee et al., 1996), thus accounting for the effect of cations on enzyme activity (Peracchi et al., 1995; Ruvinov et al., 1995a; Woehl & Dunn, 1995).

The PLP-dependent β reaction proceeds through a series of intermediates (Scheme 1A). The ϵ-amino group of βLys87 forms an internal aldimine (E) with the coenzyme PLP. The reaction of L-serine with the β-subunit is initiated by a transaldimination reaction in which the α-amino group of L-serine displaces the ϵ-amino group of βLys87 and forms an external aldimine (E-Ser) with PLP. The next steps in the synthesis of L-tryptophan involve conversion of E-Ser to aminoacrylate (E-AA) followed by addition of indole to form a quinonoid intermediate (E-Q) and protonation of E-Q to form an external aldimine (E-Trp). Kinetic studies indicate that conversion of E-Ser to E-AA in the β-subunit activates the α reaction significantly and that conformational changes in this step play roles in allosteric interactions between the α- and β-subunits (Anderson et al., 1991; Banik et al., 1995; Brzović et al., 1992b).

The mutant $\alpha_2\beta_2$ complex in which the β-subunit active site Lys87 is replaced by threonine (βK87T) has no measurable activity in reactions catalyzed by the β-subunit but retains α-subunit activity (Lu et al., 1993). The mutant enzyme forms very stable external aldimine derivatives with L-serine (E-Ser in Scheme 1B) or L-tryptophan (E-Trp in Scheme 1B) at the active site of the β-subunit. The observation that these complexes were not further converted to E-AA or E-Q (Scheme 1A) suggested that βLys87 plays a catalytic role as the acceptor of the α-proton of L-serine in the conversion of E-Ser to E-AA and as the donor of a proton in the conversion of E-Q to E-Trp in the formation of L-tryptophan. Here we describe three-dimensional structures of the mutant (βK87T) $\alpha_2\beta_2$ complex with either the substrate L-serine (βK87T-Ser) or the product L-tryptophan (βK87T-Trp) bound as an external aldimine with PLP at the active site of the β-subunit. We also present structures with L-serine bound to the β site and either GP (βK87T-Ser-GP) or IPP (βK87T-Ser-IPP) bound at the active site of the α-subunit. The results further identify the substrate and product binding sites in each subunit and provide insight into conformational changes that occur upon formation of these complexes.

MATERIALS AND METHODS

Crystallization and Data Collection. The expression and purification of the mutant (βK87T) tryptophan synthase $\alpha_2\beta_2$ complex from *Salmonella typhimurium* have been described (Miles et al., 1989; Lu et al., 1993). The βK87T-Ser and βK87T-Trp complexes were prepared by mixing the βK87T $\alpha_2\beta_2$ complex with 10 mM L-serine or 10 mM L-tryptophan. Prior to crystallization, the enzyme concentration was adjusted to 10−15 mg/mL. Crystals of the βK87T mutant containing bound L-serine or L-tryptophan were grown under the conditions used previously for crystallization of the wild-type enzyme (50 mM Bicine, 1 mM Na-EDTA, 0.8−1.5 mM spermine, and 12% PEG 8000 adjusted to pH 7.8 with NaOH) (Ahmed et al., 1985). In order to crystalize the βK87T-Ser-GP and βK87T-Ser-IPP complexes, the βK87T-Ser enzyme was cocrystallized under the identical conditions with addition of 10 mM GP or 0.4 mM IPP. These crystals belong to the space group *C*2 with the asymmetric unit being the $\alpha\beta$ pair.

Diffraction data were collected at room temperature on a Raxis IIC imaging plate system mounted on a Rigaku RU-200 rotating anode X-ray generator operating at 50 kV and 100 mA. The beam was generated using a 0.3 × 3 mm focal cup, passed through a graphite monochromator, and

Table 1: Data Collection and Refinement Statistics

	K87T-Ser	K87T-Ser-IPP	K87T-Ser-GP	K87T-Trp
data statistics				
resolution (Å)	1.9	2.04	2.5	1.9
no. of unique reflections	53755	37134	24203	50490
R_{merge} (%)	7.9	8.0	8.9	4.4
completeness (%)	90.0	76.9	91.7	84.6
	72.9 (2.0−1.9 Å)	49.4 (2.13−2.04 Å)	82.6 (2.6−2.5 Å)	46.8 (2.0−1.9 Å)
cell parameter				
a (Å)	184.2	184.2	185.7	185.8
b (Å)	61.8	61.3	62.6	62.3
c (Å)	67.8	67.9	67.9	67.8
β (deg)	94.8	94.5	94.4	94.1
refinement statistics				
resolution range (Å)	8.0−1.9	8.0−2.04	8.0−2.5	8.0−1.9
no. of reflections ($>2\sigma$)	49846	36088	23487	49681
no. of protein atoms[a]	4930	4965	4958	4965
no. of solvent				
water	254	189	128	358
cation	1 (Na^+)	1 (Na^+)	1 (Na^+)	1 (Na^+)
R-factor (%)[b]	18.6	21.4	19.3	17.1
R-factor/R_{free} (%)[c]	20.8/24.8	21.4/29.1	18.7/27.8	17.7/21.9
rms deviations from ideals				
bond length (Å)	0.016	0.014	0.014	0.016
bond angle (deg)	3.1	3.0	3.0	2.1

[a] Due to variations in the quality of the electron density, residues (1−180, 192−268 of the α-subunit, 3−391 of the β-subunit, and the serine-PLP intermediate) were modeled in the K87T-Ser structure, residues (1−187, 194−268 of the α-subunit, 3−391 of the β-subunit, the serine-PLP intermediate, and one molecule of glycerol 3′-phosphate) were modeled in the K87T-Ser-GP structure, and residues (1−187, 194−268 of the α-subunit, 3−391 of the β-subunit, the serine-PLP intermediate, and one molecule of indole-3-propanol phosphate) were modeled in the K87T-Ser-IPP structure. The K87T-Trp structure is composed of residues 1−178, 192−268 of the α-subunit, 3−397 of the β-subunit, and the tryptophan-PLP intermediate. [b] *R*-factor value of each structure has been calculated using all reflections from the given resolution. [c] After structural determination was completed, *R*-factor and R_{free} were calculated by a simulated annealing refinement using 90% and 10% of reflections from the given resolution, respectively, to assess the quality of the final model.

collimated using a 0.35 mm collimator. The oscillation axis was either along or perpendicular to the *b*-axis of the crystal with an oscillation range of 1.2−2.0°. All diffraction data were processed with the software from RIGAKU.

Structure Determination of the βK87T-Ser, βK87T-Trp, βK87T-Ser-IPP, and βK87T-Ser-GP $\alpha_2\beta_2$ Complexes. Crystals of the four complexes all were grown under similar conditions, varying only in the presence or absence and concentrations of substrates or inhibitors. The cell parameters, data statistics, and refinement statistics are summarized in Table 1. In every case, a lack of isomorphism presumably due to conformational changes and small changes in cell constants (see below) precluded the wild-type structure[2] from serving as a direct phasing model for refinement. Better convergence during refinement required the application of rigid-body refinement and simulated annealing refinement with X-PLOR (Brünger, 1992). In two cases, the program PROLSQ (Cohen, 1986; Hendrickson & Konnert, 1981; Hendrickson, 1985; Sheriff, 1987) was used in the final stages of refinement.

For the K87T-Trp structure, a difference map of the K87T-Trp complex vs the wild-type enzyme, calculated using phases from the refined model of the wild-type enzyme, indicated the presence of the PLP-tryptophan complex bound in the β-subunit active site. Other features in the difference map were indicative of large movements in the protein, particularly in the N-terminal domain (residues 3−52, 86−204) of the β-subunit. The clarity of the difference map and the $2F_o - F_c$ map was dramatically improved through a series of rigid-body and simulated annealing refinements with X-PLOR. The refined wild-type model at 2.5 Å resolution (Hyde et al., 1988) was divided into three substructures (corresponding to the α-subunit and the N- and C-terminal domains of the β-subunits) and truncated by removing regions of high mobility (residues α55−61, α178−191, β135−144, β159−175) prior to rigid-body refinement. Two subsequent cycles of simulated annealing refinement, followed by manual rebuilding using computer graphics, resulted in a clear, 1.9 Å resolution $2F_o - F_c$ map in which the conformation of the PLP-tryptophan external aldimine was evident. An atomic model corresponding to the external aldimine was fitted to the electron density and refined in nine rounds of refinement using PROLSQ, interspersed with graphics fitting and rebuilding using the program CHAIN. Temperature factor refinement was altered with positional refinement. Ideal stereochemical restraints applied to the external aldimine model of L-tryptophan in the PROTIN program dictionary were derived from an energy-minimized model constructed with QUANTA. The final refined model yields a standard *R*-factor of 17.1% at 1.9 Å resolution (Table 1). One Na^+ atom and 358 water molecules are included. Disordered residues that could not be modeled include residues α179−191 (loop 6) and β1−2. Residue βGlu334 showed bifurcated side chain density and was refined in two discretely disordered conformations.

The starting model for the refinement of the βK87T-Ser structure consisted of a similar truncated version of the wild-type enzyme structure divided into rigid-body domains. The model was subjected to four cycles of rigid-body and simulated annealing refinement and alternating cycles of positional and temperature factor refinement. The resulting $2F_o - F_c$ and $F_o - F_c$ maps using phases calculated from the partially refined model allowed many of the solvent atoms and residues that were excluded from the starting model to be modeled (footnote, Table 1). The PLP-serine external aldimine in the β active site was identified unambiguously,

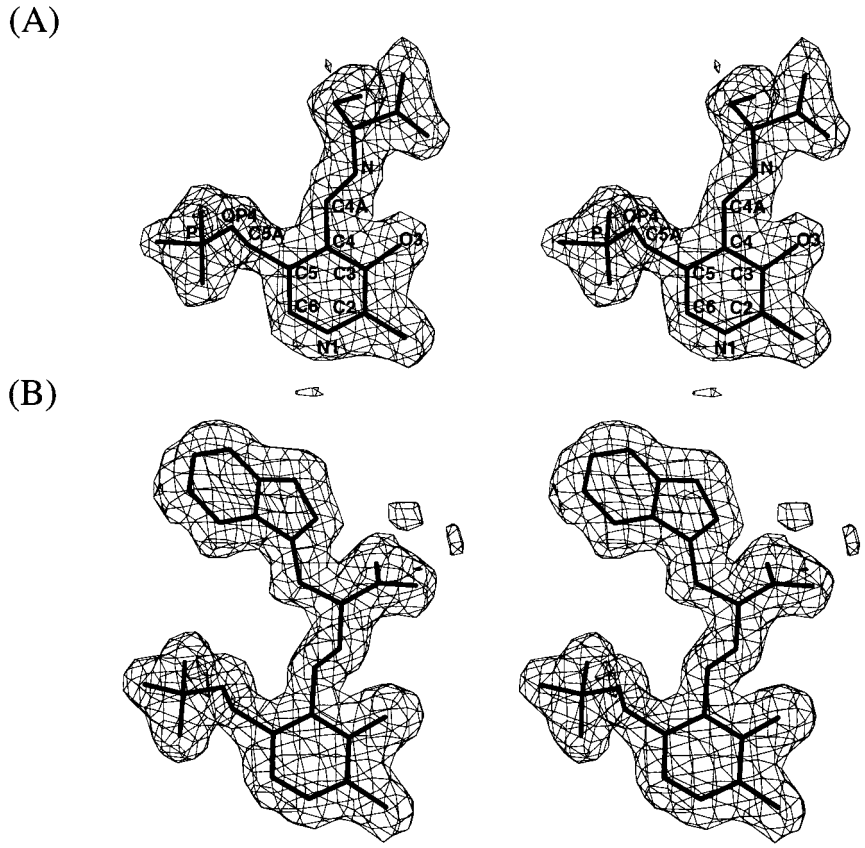

FIGURE 1: Final $2F_o - F_c$ map overlaid on the models of the external aldimines of the coenzyme pyridoxal 5′-phosphate with (A) L-serine in the βK87T-Ser structure and with (B) L-tryptophan in the βK87T-Trp structure. The map was contoured at 1σ. The numbering of the positions in the coenzyme is shown in (A). Note that the carboxylates of L-serine and L-tryptophan have different orientations.

modeled, and refined with PROLSQ to yield a crystallographic *R*-factor of 18.6% at 1.9 Å resolution. No density for α-subunit loop 6 was visible.

A preliminary difference map calculated between diffraction data sets from the βK87T-Ser-GP complex and βK87T-Ser (above), using phases from the refined βK87T-Ser structure, was noisy, suggesting that GP caused extensive structural perturbations. The βK87T-Ser structure from above was used as a starting model for refinement using X-PLOR following a similar division into three rigid body domains (the α-subunit and the β-subunit N- and the C-terminal domains). Rigid-body refinement resulted in a significant decrease of the crystallographic *R*-factor from 48.3% to 35.4%. Standard simulated annealing, positional, and isotropic temperature factor refinement further decreased the *R*-factor to 23.8%. A newly calculated $F_o - F_c$ Fourier map revealed the PLP-serine external aldimine complex in the β-subunit and GP in the α-subunit. An idealized model of GP was modeled using QUANTA and fitted to the density. Although only the D-enantiomer of G3P is produced in the reaction catalyzed by the α-subunit (Crawford, 1960), the L- and D-enantiomers of GP could not be distinguished in the electron density and were both modeled. An important new structural feature appearing near the bound GP was density corresponding to most of loop 6 in the α-subunit, residues 179−187. Residues α188−193 were still highly disordered and could not be modeled. A total of 128 water molecules and one Na^+ were introduced during rebuilding with the program O (Jones et al., 1991). The structure of βK87T-Ser-IPP complex was determined using a nearly identical approach. Here, too, residues α179−187 could be included in the final model (Table 1).

Structural Comparisons. Conformational differences between these four structures have been assessed by comparing each structure with the 1.9 Å refined wild-type structure,[2] using a superposition method developed by Lesk (1991) and Gerstein and Chothia (1991). The backbone atomic coordinates of all residues (residues 3−391) in the β-subunit from the wild-type structure were superimposed in pairs on the βK87T-Ser, βK87T-Ser-GP, βK87T-Ser-IPP, or βK87T-Trp structure, resulting in overall rms deviations of 0.44, 1.15, 0.94, and 1.17 Å, respectively. Residues having rms deviations of 2.0 Å or more were not included in the next superposition cycle. Several more cycles of superposition were carried out with a smaller threshold until none of the superimposed residues had a deviation of more than 0.4 Å. Due to a relatively large difference in a resolution between the wild-type (1.9 Å) and βK87T-Ser-GP (2.5 Å) structures, a higher final threshold of 0.6 Å was used for the superposition of these two structures. The iterative superpositions yielded a basis set of "core residues" of the β-subunit that were used to align the βK87T-Ser, βK87T-Ser-GP, βK87T-Ser-IPP, or βK87T-Trp structure with the wild-type structure (see Table 3). The core residues contain mainly residues from the C-terminal domain. The main chain deviations in the corresponding residues of the wild-type and mutant structures were determined in each pair of superimposed structures.

RESULTS

Structures of External Aldimines at the Active Site of the β-Subunit. The electron density maps and the final models for the external aldimines of PLP with L-serine and L-tryptophan in the βK87T-Ser and βK87T-Trp $\alpha_2\beta_2$ com-

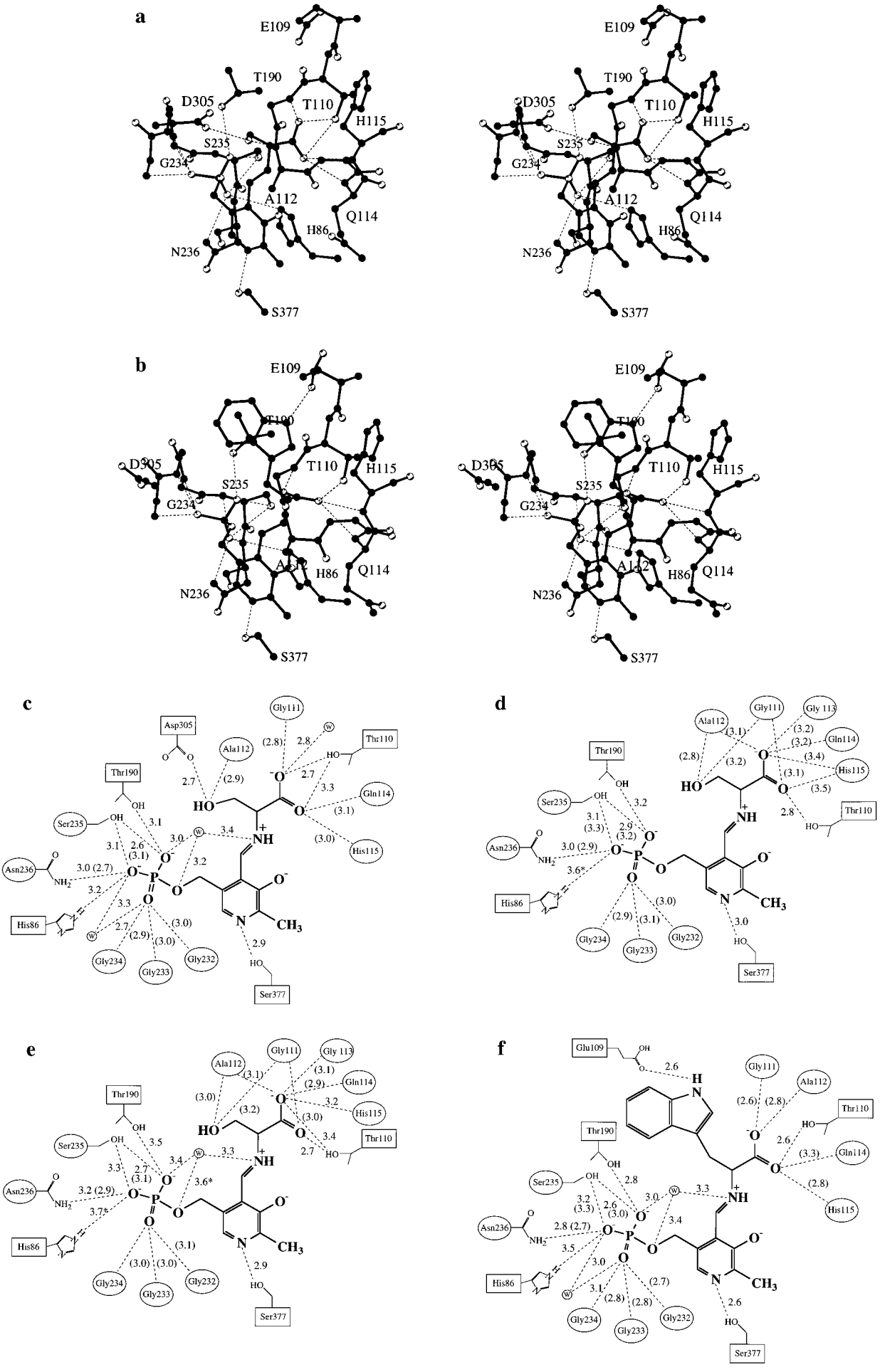
a
E109
T190
D305
T110
H115
S235
G234
A112
Q114
H86
N236
S377
b
c
Asp305
Gly111
Ala112
Thr110
Thr190
Gln114
Ser235
His115
Asn236
His86
Gly234
Gly233
Gly232
Ser377
d
Gly 113
Gln114
e
f
Glu109

FIGURE 2: Interactions between polar atoms of the external aldimines and protein residues within 3.5 Å in the β-subunit of the four complexes. Stereo diagrams of the active site of (a) the βK87T-Ser and (b) the βK87T-Trp structures. Open circles represent oxygen atoms; other atoms are represented by filled circles. Dashed lines indicate polar interactions. Schematic diagrams of the active site of (c) the βK87T-Ser, (d) the βK87T-Ser-IPP, (e) the βK87T-Ser-GP, and (f) the βK87T-Trp structures. Residues are enclosed with an oval if their main chain atoms interact with polar atoms (oxygen or nitrogen) of the external aldimine or with a rectangle if their side chains alone contribute to polar interactions. If both the main chain and side chain atoms form interactions with the external aldimines, residues with the side chain are in an oval (see Ser235 and Asn236). Corresponding interactions are indicated with dashed lines. The numbers correspond to interatomic distances in angstroms formed by the main chain atoms (in parentheses) or by the side chain atoms (without parentheses). Each water molecule is labeled with W in a small circle. An asterisk indicates an interaction more than 3.5 Å.

plexes are shown in Figure 1. The high quality of the electron density permits PLP and its associated amino acid to be located precisely. The conformations of the external aldimines of PLP with L-serine in the βK87T-Ser-IPP and βK87T-Ser-GP complexes are almost identical to that of the βK87T-Ser complex (see below). Figure 2 shows the polar interactions within 3.5 Å between the external aldimines and the protein residues in the β-subunit in the four structures. The binding environments of PLP are closely similar in the four structures, but there are some minor differences when tryptophan is bound to the coenzyme. The indole side chain displaces three water molecules from the active site that are observed in the presence of L-serine. There are also differences in conformation of the carboxylate groups of L-serine and L-tryptophan, mainly as the result of rotation along the Cα−N and Cα−C bonds (Figures 1 and 2a,b). These differences are probably due mainly to steric hindrance between the bulky side chain of tryptophan and the carboxyl oxygens. Placing these oxygens in the same conformation as in the serine complex results in close contacts with the indole group in a range of 2.9−3.2 Å. Although this rotation displaces the positions of the carboxylate oxygens by 0.7 and 2.3 Å, the carboxylate groups of L-serine and L-tryptophan have similar interactions with the active site residues (Figure 2c,f). The main differences are observed near the side chain of the bound amino acid. In the βK87T-Ser structure, the side chain hydroxyl group of L-serine forms a hydrogen bond (distance of 2.7 Å) to the side chain carboxylate of βAsp305 (Figure 2a,c). In the βK87T-Ser-IPP, βK87T-Ser-GP, and βK87T-Trp structures the side chain of βAsp305 has a different orientation. It does not interact with the serine hydroxyl group (Figure 2b,d−f) but rather swings out to ion pair with βArg141.

Figure 3 shows the external aldimines of PLP with L-serine and L-tryptophan from three structures with the βK87T mutation and of the internal aldimine between PLP and βLys87 from the wild-type structure (Hyde et al., 1988). The phosphates are located at nearly identical positions in all the structures. The conversion of the internal aldimine to the external aldimine results in a tilt of the planar coenzyme ring by about 10°, compared to a tilt of about 27° in various isozymes of the PLP-dependent aspartate aminotransferase (Jansonius & Vincent, 1987).

Loop 6 Is Ordered When Both Active Sites Are Occupied. We have located IPP and GP at the α-subunit active site in the βK87T-Ser-IPP and βK87T-Ser-GP structures, respectively (see Figures 4 and 5). In these two structures, residues 179−187 of the α-subunit loop 6, which connects strand 6 with helix 6, assume an ordered conformation (Figure 4A). This loop is disordered in the wild-type structure with and without IPP (Hyde et al., 1988) and is also disordered in the βK87T-Ser and βK87T-Trp structures. Thus, the combined presence of ligands at the active sites of both α- and β-subunits appears to be necessary for the stabilization of

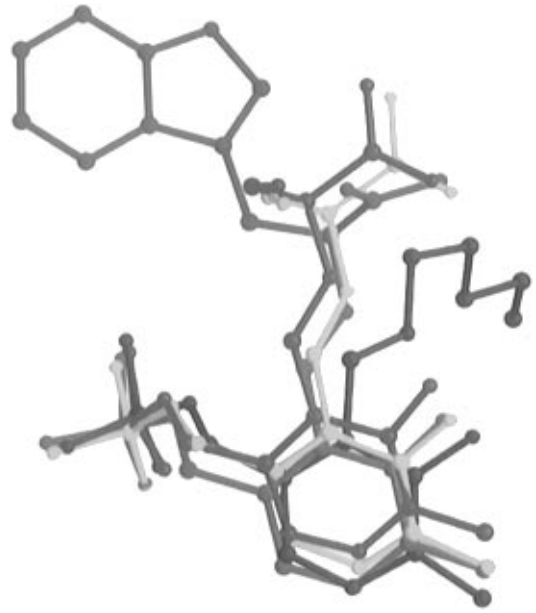

FIGURE 3: Diagrams showing positions of the coenzyme pyridine ring in the internal aldimine and in the three external aldimines. The internal aldimine in the wild-type structure is in magenta, the external aldimine in the βK87T-Ser is in red, the external aldimine in the βK87T-Ser-GP is in yellow, and the external aldimine in the βK87T-Trp structure is in green. The external aldimine in the βK87T-Ser-IPP is not shown because it is almost identical to that in the βK87T-Ser-GP structure. The phosphate group occupies approximately the same position in each intermediate.

loop 6. This conclusion is consistent with the previous finding that the presence of L-serine at the β site and GP at the α site almost completely protects loop 6 from tryptic cleavage whereas the presence of GP alone provides only partial protection (Miles, 1991b; Ruvinov & Miles, 1992).

Figure 4A shows the electron density map for IPP and the loop 6 residues α179−187 in the βK87T-Ser-IPP structure. An almost identical conformation of loop 6 is also observed in the βK87T-Ser-GP structure. Panels B and C of Figure 4 show the density for the GP modeled with the D- and L-enantiomers. This complex was crystallized with D/L-α-glycerol 3-phosphate, and it is not evident from the difference map whether the D-enantiomer alone (analogous to the natural product D-glyceraldehyde 3-phosphate) or a mixture of the D- and L-enantiomers are bound to the active site. Both enantiomers fit the density and give the same crystallographic *R*-values.

Surface area calculations (Connolly, 1983) with a probe radius of 1.4 Å show that loop 6 closes the active site of the α-subunit in the βK87T-Ser-IPP and βK87T-Ser-GP structures, burying a total area of 350 Å^2. Loop 6 makes about 14 van der Waals contacts with the bound IPP or GP, while the only polar interaction is a long-range hydrogen bond (about 3.5−3.7 Å) between αGly184 and a phosphate oxygen of IPP or GP. With loop 6 in this position, αThr183 forms

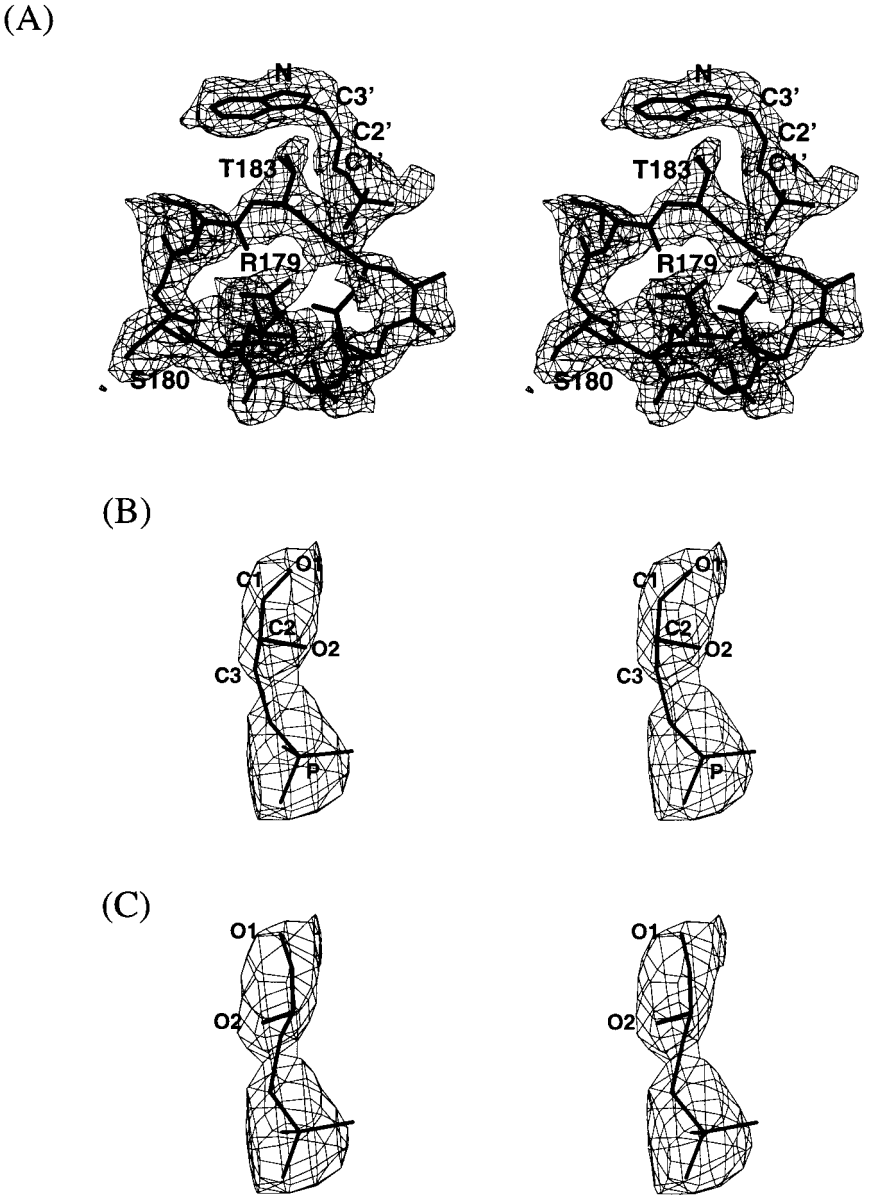

FIGURE 4: $2F_o - F_c$ maps overlaid on the final models of (A) indole-3-propanol phosphate and residues in loop 6, (B) D-α-glycerol 3-phosphate, and (C) L-α-glycerol 3-phosphate. Phases are calculated from the final model, and maps are contoured at the 0.8σ level in (A) and the 1.0σ level in (B) and (C).

a hydrogen bond with αAsp60, which is believed to play a catalytic role in the α reaction (see Discussion). Despite the many contacts between loop 6 and the rest of the enzyme (Table 2), there is still evidence for a high degree of residual flexibility; residues 188−193 are very disordered and are not visible in the electron density, and residues 186−187 have high temperature factors (∼80 Å^2).

Panels A and B of Figure 5 show the binding environments for IPP and the D-enantiomer of GP, respectively. In this orientation it is apparent that loop 6 effectively covers the bound IPP and GP and isolates the active site of the α-subunit from solvent. The binding site of IPP in the βK87T-Ser-IPP structure is essentially identical to that originally observed for the IPP in the wild-type structure (Hyde et al., 1988). The nitrogens of αGly213, and of αGly234, and the main chain nitrogen and the side chain hydroxyl oxygen of αSer235 are within possible hydrogen-bonding distances (less than 3.5 Å) from the phosphate oxygens of IPP. The side chain of αArg179 in loop 6 is in the general vicinity of the negatively charged phosphate group of IPP, but the electron density clearly indicates that the guanidinium group is pointing away (about 5.5 Å) from the phosphate group and instead interacts with other backbone oxygens of near residues (see Discussion). The carboxylate of αAsp60 is oriented toward the indole nitrogen at a distance of about 2.8−3.3 Å.

Contacts similar to those observed in IPP are also found around GP in the βK87T-Ser-GP structure. The phosphate group in each enantiomer of GP has polar interactions with the nitrogen of αGly184, the nitrogens of αGly213 and of αGly234, and the main chain nitrogen and the side chain hydroxyl oxygen of αSer235. The models for both enantiomers show that the phenolic hydroxyl of αTyr175 is within hydrogen-bonding distance (about 2.9 Å) of the hydroxyl oxygen (O1) on C1 of L- or D-GP (Figure 5B). No polar contacts are observed between the hydroxyl oxygen (O2) on C2 and any protein residues in either model.

Comparison of the Wild-Type and Mutant Structures. The conformation of each mutant structure was compared with the wild-type structure following superposition of the core

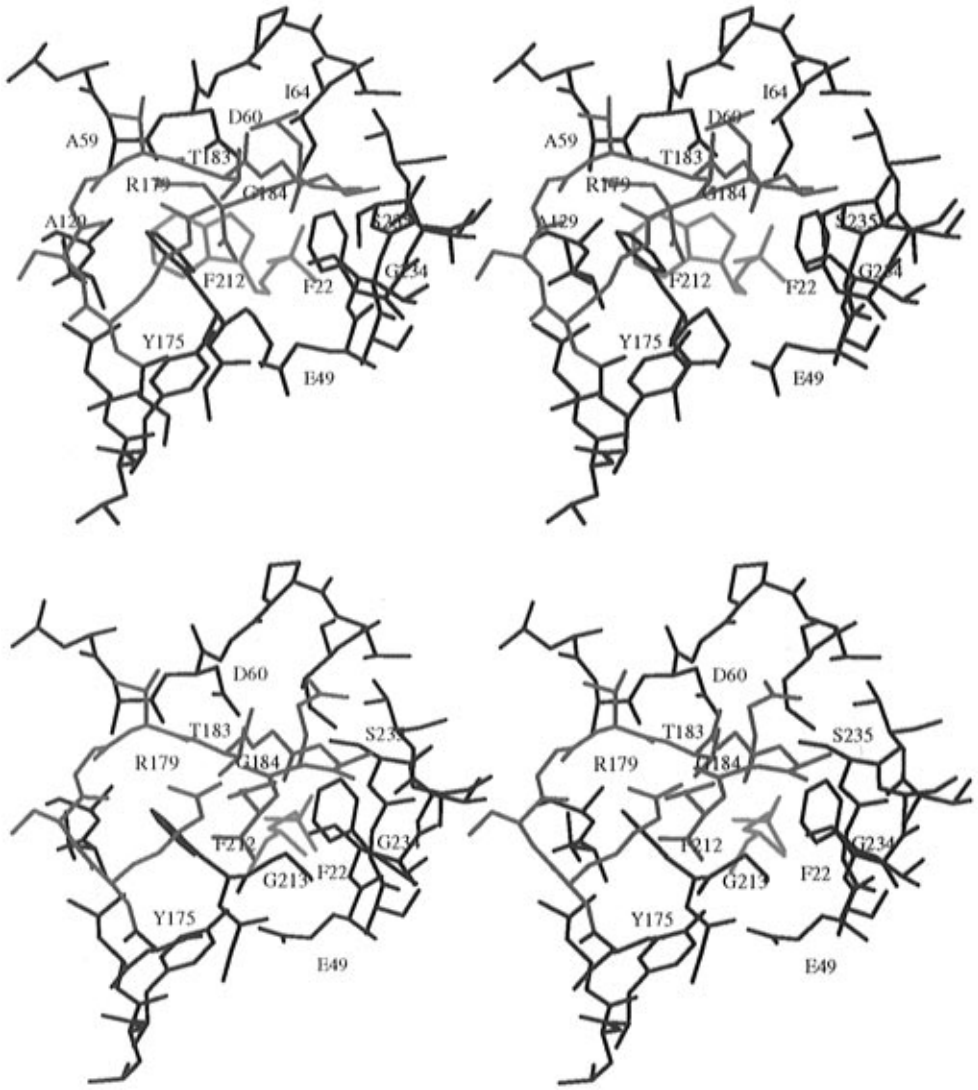

FIGURE 5: Binding site for (A, top) indole-3-propanol phosphate and (B, bottom) D-α-glycerol 3-phosphate in the α-subunit. Indole-3-propanol phosphate and D-α-glycerol 3-phosphate are colored in green and residues in loop 6 in red. Residues within 4.0 Å from the bound substrate analogs are labeled. αGlu49 and αArg179 are labeled due to their possible roles in catalysis (see Discussion).

Table 2: Polar Interactions between Residues in Loop 6 and the Remaining Residues in the *β*K87T-Ser-IPP and *β*K87T-Ser-GP Structures

residues in loop 6		distance (Å)	interacting residues	
(A) *β*K87T-Ser-IPP				
αSer178	O*γ*	2.9	αGln210	O*ϵ*1
αSer178	O	2.7	αPhe212	O
αThr183	N	3.1	αAla59	O
αThr183	N	3.5	αGly61	N
αThr183	O*γ*1	2.8	αAsp60	O*δ*1
αThr183	O*γ*1	2.9	αGly61	N
αThr183	O	3.4	αGly61	N
(B) *β*K87T-Ser-GP				
αSer178	O*γ*	2.6	αPhe212	N
αSer178	O*γ*	2.7	αPhe212	O
αSer180	O*γ*	3.3	*β*Tyr181	OH
αThr183	N	3.1	αAla59	O
αThr183	O*γ*1	2.8	αAsp60	O*δ*1
αThr183	O*γ*1	3.4	αGly61	N
αThr183	O	3.1	αGly61	N
αGly184	N	3.5	GP	OP2
αGly184	O	3.5	GP	OP3
αAla185	O	3.4	αSer215	O*γ*

Table 3: Summary of Superpositions between the Wild-Type Structure and Each of the Liganded Mutant Structures

	K87T-Ser	K87T-Ser-IPP	K87T-Ser-GP	K87T-Trp
no. of residues in the *β*-subunit	389	389	389	389
no. of defined core residues[a] after superposition	296	221	119	195
overall rms deviation of the core residues (Å)	0.18	0.22	0.26	0.19
rotation of the α-subunit[b] relative to the *β*-subunit (deg)	0.3	3.1	4.9	4.0

[a] The core residues are defined as those in the *β*-subunit showing rms deviations of the backbone atoms less than 0.4 or 0.6 Å (see Materials and Methods). [b] Rotation angles of the α-subunit in each mutant structure are those angles required to superimpose the α-subunit of the wild type after the mutant and wild-type structures are superimposed on the basis of the core residues of the *β*-subunit.

residues of the *β*-subunit (Table 3). The rms differences in position for each residue are shown by the solid lines in Panels A and B of Figure 6 for the α- and *β*-subunits, respectively. The *β*K87T-Ser structure shows small deviations for the α-subunit (Figure 6A) and modest changes for the *β*-subunit (Figure 6B). In contrast, larger movements in both the α- and *β*-subunits (up to 5 Å) are observed for the *β*K87T-Ser-IPP, *β*K87T-Ser-GP, and the *β*K87T-Trp structures. The largest movement of the α-subunit occurs

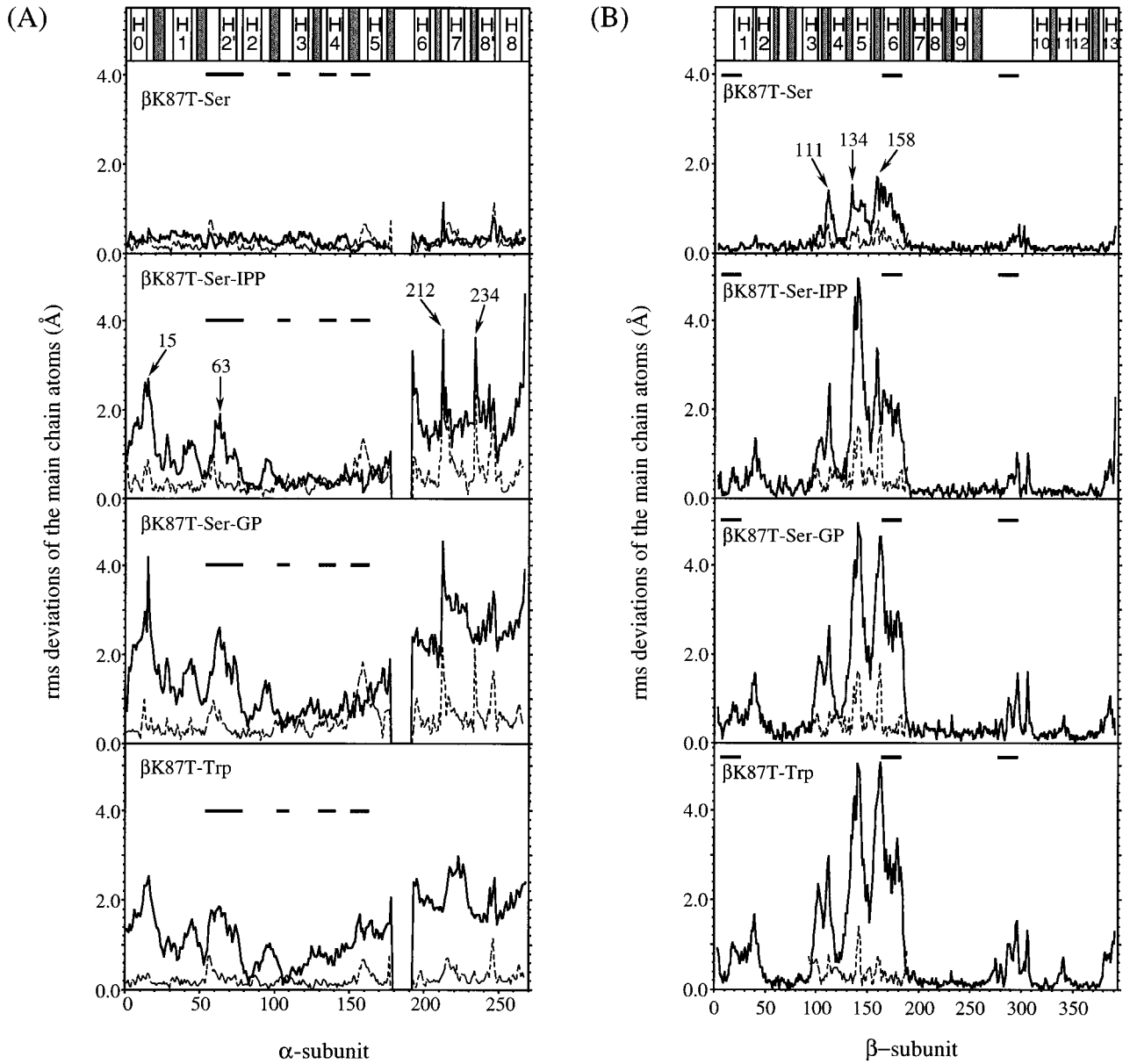

FIGURE 6: Plots showing the rms deviation in the main chain atoms for corresponding residues between each mutant and wild-type $\alpha_2\beta_2$ complex in (A) the α-subunit and (B) the β-subunit. The solid line represents rms deviations which are calculated after the β-subunit core residues have been superimposed, and the dashed line represents rms deviations of each residue after the α-subunit or the mobile region of the β-subunit is superimposed (see text for details). Secondary structural elements are indicated above the top panels with the nomenclature of Hyde et al. (1988). In the α-subunit (A), there are 11 helices as indicated by H0 to H8 and eight strands as indicated with shaded areas. In the β-subunit (B), 13 helices and 10 strands are defined. Four solid bars in (A) and three in (B) correspond to the interface residues between the α- and β-subunits (see Results and Figure 9 for details).

for the βK87T-Ser-GP structure which undergoes a displacement that can be represented as a rigid-body rotation of approximately 5° about an axis (see Table 3) that passes through residues αLeu85 in the middle of helix 2 and αVal106 in a loop between strand 3 and helix 3 (Figure 7A). The overall rms deviation of the α-subunit (as represented by the dashed line in Figure 6A) is only 0.24 Å for the βK87T-Ser, 0.65 Å for the βK87T-Ser-GP, 0.69 Å for the βK87T-Ser-IPP, and 0.33 Å for the βK87T-Trp structures, suggesting that the overall tertiary structures of the α-subunit in each of the mutant structure complexes are well preserved. Notable localized differences occur in the phosphate binding site residues, notably αPhe212 and αGly213 in loop 7 between helix 7 and strand 7 (Figure 6A). The side chain of αPhe212, commonly disordered when loop 6 is disordered, is fixed in position underneath loop 6 in the closed conformation.

Changes in the β-subunit residues can also be described largely in terms of a rigid-body rotation of part of the N-terminal domain, residues 93−189, by 10° relative to the rest of the β-subunit, effectively moving these two regions closer together. This mobile subdomain includes the core region of the N-domain (residues 86−135 and 140−190) which is structurally homologous to a corresponding core region in the C-domain (residues 204−260 and 306−377) (Hyde et al., 1988). There are no major overall changes in tertiary structure for the mobile region in the β-subunit, except for residues 137−141 in helix 5 and residues 160−163 in a loop between strand 5 and helix 6. Similar rotations of the α-subunit and of the mobile region in the β-subunit

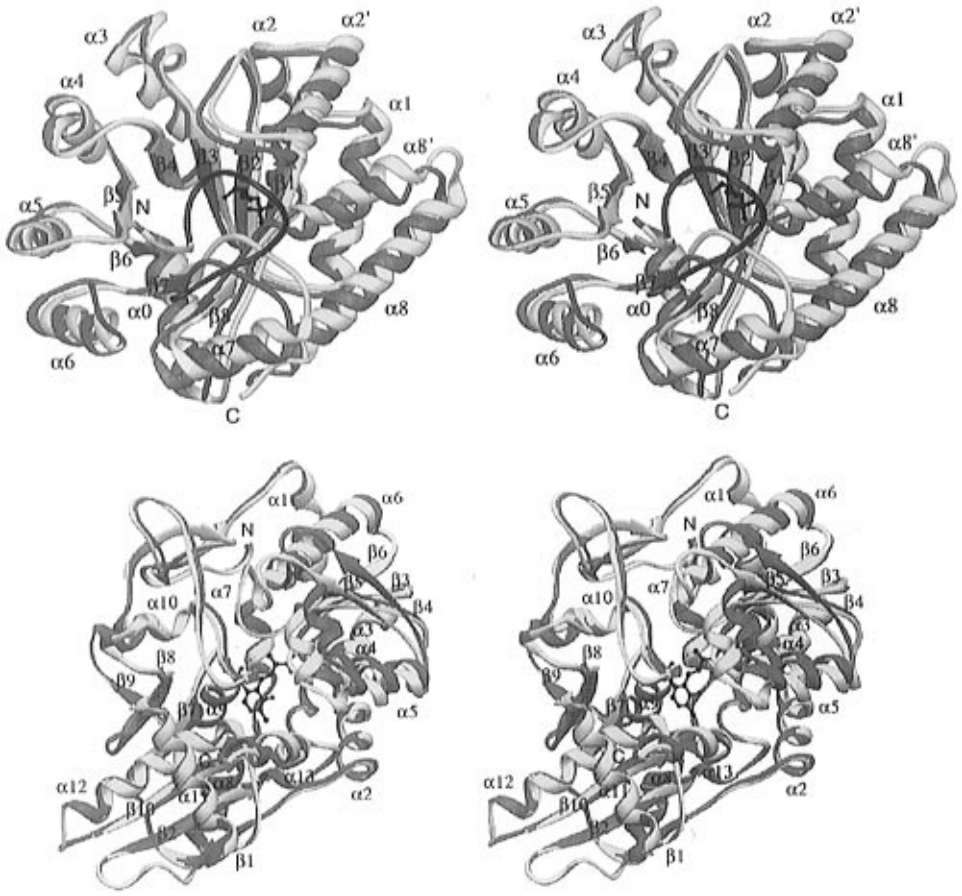

FIGURE 7: Conformational changes between the wild-type enzyme (red) and the *β*K87T-Ser-GP mutant complex (yellow). In these ribbon diagrams (Carson, 1987) the core residues of the *β*-subunit were superimposed as described in Table 3. (A, top) The α-subunit. The large positional differences are the result of a rotation of the α-subunit relative to these core residues. Loop 6 (residues 179−187 in blue) as localized in the *β*K87T-Ser-GP structure covers the GP (black) bound to the active site. (B, bottom) The *β*-subunit. The mobile region (residues 93−189: α3−α6 and *β*3−*β*6) is on the right side and contains most of the N-terminal domain. The *β* active site is located at the interface between this region and the rest of the *β*-subunit. The external aldimine in the *β*K87T-Ser-GP structure is indicated with black.

Table 4: Buried Surface Area between the Mobile Region[a] and the Rest of the *β*-Subunit in the Wild-Type and Liganded Mutant Forms of Tryptophan Synthase

	wild type	K87T-Ser	K87T-Ser-IPP	K87T-Ser-GP	K87T-Trp
buried surface area (Å^2)	1330	1540	1760	1740	1780
differences in the buried surface area[b] (Å^2)		210	430	410	450

[a] Residues from Gly93 to Gly189 are defined as the mobile region. [b] Differences are calculated as surface area$_{\text{liganded mutant}}$ − surface area$_{\text{wild type}}$.

are observed in the *β*K87T-Ser-IPP and *β*K87T-Trp structures (Figure 6 and Table 3).

Interface between the N- and C-Domains of the β-Subunit. The movement of the mobile region (residues 93−189) of the N-terminal domain toward the C-terminal domain of the *β*-subunit (Figures 6B and 7B) causes a diminution in the volume of the tunnel joining the α and *β* active sites and results in an increase in the buried surface area between these regions (Table 4). The changes are relatively small for the *β*K87T-Ser structure but more dramatic for the other three structures. Associated with these movements are some changes in the interatomic distances between the mobile region and the rest of *β*-subunit (Table 5, Figure 8). Interactions involving residues *β*Arg141, *β*Gln142, *β*Arg148, and *β*Lys167 show large differences; for *β*Lys167 the difference is the result of a change in side chain orientation in the four mutant *β*K87T complexes, not from a change in main chain conformation. Residues *β*Arg141, *β*Gln142, and *β*Arg148 move significantly closer to the C-terminal domain residues *β*Asp305, *β*Lys382, *β*Asp383, and *β*Thr386 (Figure 8B).

Geometry of the Tunnel in the Mutant Structures. The hydrophobic tunnel that connects the active sites of the α- and *β*-subunits is principally located between the N- and C-terminal domains of the *β*-subunit and is believed to provide a mechanism for indole channeling (Hyde et al., 1988). Subsequent refinement at higher resolution of the wild-type structure[2] reveals two sites at which the tunnel is partly blocked. In the first, the side chain of *β*Phe280 is inserted directly into the tunnel, although the density for the side chain is weak, suggesting either dynamic or static disorder. A previous analysis of the wild-type complex in the presence of different monovalent cations revealed that in the presence of K^+ and Cs^+ the *β*Phe280 side chain did in fact move out of the tunnel and was repositioned on the surface of the tunnel (Rhee et al., 1996). This rearrangement supports the hypothesis that the *β*Phe280 may act as a gate to influence the free diffusion of indole.

The second site involves the side chain of αLeu58, which in all of the structures that we have hitherto observed is inserted into the side of the tunnel, partly restricting the

Table 5: Polar Interactions between the Mobile Region[a] and the Rest of the β-Subunit and Their Distances in the Wild-Type and Liganded Mutant Forms of Tryptophan Synthase

mobile region		interacting residues		distance (Å)[b]				
residue	atom	residue	atom	wild type	K87T-Ser	K87T-Ser-IPP	K87T-Ser-GP	K87T-Trp
Gln94	Nϵ2	Gln90	Oϵ1	3.5	3.5	(4.9)	(5.0)	(3.8)
	Nϵ2	Gln90	Nϵ2	2.7	2.8	3.2	3.0	2.9
Arg100	O	Arg34	Nη1	3.2	3.4	3.5	(5.1)	(5.4)
	Nη1	Asp38	Oδ1	3.4	3.2	3.5	2.9	(5.1)
	Nη2	Asp38	Oδ1	2.8	2.4	3.0	2.7	3.0
Lys103	Nζ	Gln27	Oϵ1	3.3	3.1	3.5	(4.2)	(3.7)
Gln114	Nϵ2	Gly83	O	(4.0)	(4.0)	2.7	2.8	3.0
Arg141	O	Thr386	Oγ1	(7.8)	(7.0)	3.3	3.3	3.1
	Nη1	Asp305	Oδ2	(7.4/6.2)[c]	(7.2)	3.1	2.8	2.8
	Nη2	Ser299	O	(7.4)	(7.1)	3.3	3.1	2.7
	Nη2	Ile300	O	(8.1)	(8.0)	(4.2)	(3.6)	(3.6)
Gln142	Oϵ1	Lys382	Nζ	(8.5)	(6.8)	(3.8)	(4.7)	2.8
	Nϵ2	Lys382	O	(7.4)	(7.6)	(3.8)	(3.9)	3.5
	Nϵ2	Asp383	Oδ1	(8.0)	(7.8)	(3.6)	3.4	2.9
Arg148	Nη1	Gly83	O	(9.0)	(8.7)	2.9	3.3	2.9
	Nη2	Gly83	O	(7.8)	(6.5)	3.2	2.8	3.0
Ser163	N	Glu296	Oϵ2	(7.4)	(6.0)	(6.0)	3.5	3.5
Lys167	O	Tyr279	Oη	(6.2)	3.1	3.4	(3.6)	3.5
	Nζ	Asp305	O	3.3	(9.8)	(8.9)	(9.1)	(8.8)
	Nζ	Asp305	Oδ2	2.8	(11.6)	(9.7)	(9.4)	(9.4)
Asn171	Oδ1	Tyr279	Oη	(7.3)	2.8	2.9	3.0	2.7
Tyr186	O	Tyr197	Oη	2.7	2.8	2.7	2.8	2.6
Leu188	O	Gln90	Oϵ1	3.3	3.1	2.6	2.7	3.1

[a] Residues from Gly93 to Gly189 are defined as the mobile region. [b] Interatomic distances of less than 3.5 Å between polar atoms are considered as polar interactions, and interactions beyond this limit value are enclosed in parentheses. [c] The side chain of βAsp305 has two rotameric states in the wild-type structure (Rhee et al., 1996).

passage of indole. However, in the wild-type structure this region, from residues 54 to 61, which includes the catalytic residue αAsp60, is the most mobile part of the α-subunit with *B*-values ranging from 40 to 60 Å^2, suggesting that its dynamics may too play a role in the diffusion of indole. In the four structures described here there is fairly clear density corresponding to the side chains of αLeu58 and βPhe280, with the side chain of βPhe280 completely blocking the tunnel (Figure 9).

Interface between the α- *and* β*-Subunits.* Interface residues between the α- and β-subunits are defined as those having surface area buried by association of the α- and β-subunits in the wild-type $\alpha_2\beta_2$ complex. Figure 10 schematically represents those interface residues, their relative locations, and number of contacts within 4.0 Å in the wild-type structure. Figure 10 also shows the interface residues of loop 6 of the α-subunit in the βK87T-Ser-IPP and βK87T-Ser-GP structures. These subunit interface residues and interactions in the mutant structures do not differ greatly from those in the wild-type $\alpha_2\beta_2$ complex.

A comparison of the wild-type and mutant structures in this region reveals relatively large positional changes in only two groups of interface residues (α53−78 and β161−181; see solid bars in Figure 6). The calculated buried surface area of the α−β interface does not differ significantly in any of the structures. The contribution of each cluster of interface residues to the buried area also remains approximately constant in the wild-type and mutant structures. In the βK87T-Ser-GP structure there are concerted movements of the α-subunit and of the mobile region of the β-subunit in which the interface residues α53−78 (including helix α2′) and β161−181 (including helix α6) move in the same direction (Figure 8B). Thus, the interactions between these interface residues are relatively unchanged despite large positional changes.

Two residues, however, βLys167 and βArg175, are involved in large changes in their interactions with other residues. These changes result from notable differences in the orientations of the side chains of these two β-subunit residues in the wild-type $\alpha_2\beta_2$ complex and in the four mutant βK87T structures. In the four mutant structures the side chain of βLys167 is now within hydrogen-bonding distance of the carboxylate of αAsp56, and βArg175 also interacts with the backbone oxygen of α-subunit residue Pro57 (Figure 8B).

Cation Binding Site. The sodium binding site in each of the four mutant structures is the same as that previously observed in the refined structure of the wild-type $\alpha_2\beta_2$ complex[2] (Rhee et al., 1996). It is located about 8 Å from the PLP phosphate group and near the wall of the tunnel. Exchange of K^+ or Cs^+ for Na^+ at this site induces local and long-range changes in the three-dimensional structure of the wild-type tryptophan synthase $\alpha_2\beta_2$ complex (Rhee et al., 1996).

DISCUSSION

Active Site and Catalytic Mechanism of the α*-Subunit: A New Role for Loop 6.* The active site of the α-subunit has been located by binding the substrate analog IPP in the wild-type structure (Hyde et al., 1988) and the analogs IPP and GP in the βK87T-Ser-IPP and βK87T-Ser-GP structures (Figure 5). Superposition of the α-subunits in the βK87T-Ser-IPP and βK87T-Ser-GP structures results in an overall rms deviation of 0.61 Å for the main chain atoms, indicating that most of the α-subunit residues have essentially the same positions. Comparison of the active sites confirmed that there is no rearrangement of these residues. The crystal structure (Hyde et al., 1988) and mutagenesis studies (Nagata et al., 1989; Shirvanee et al., 1990; Yutani et al., 1987) led to the proposal that the proton-transfer steps during cleavage

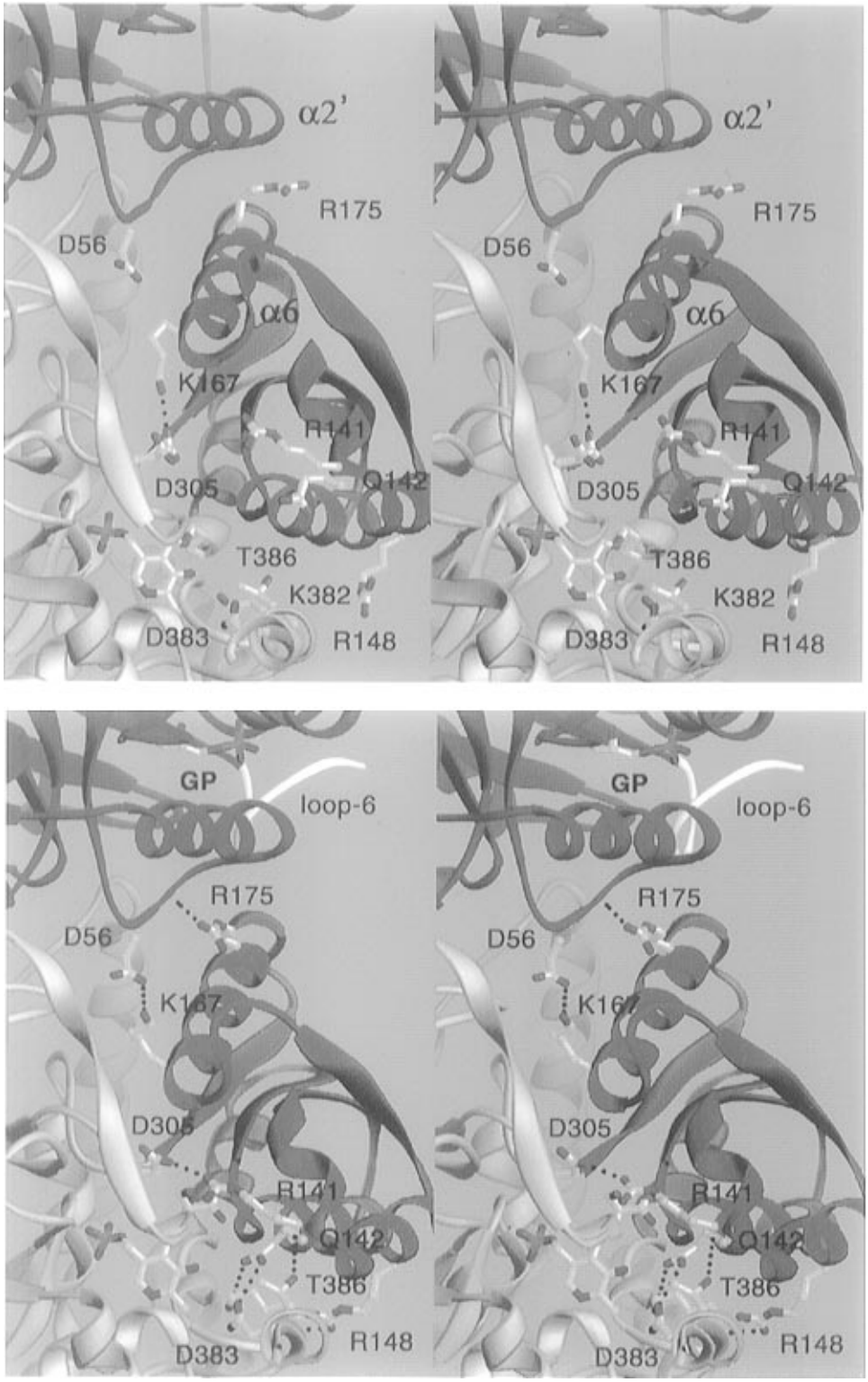

FIGURE 8: Changes in hydrogen-bonding interactions resulting from conformational differences between the (A, top) wild-type and (B, bottom) βK87T-Ser-GP $\alpha_2\beta_2$ complexes. Color codes are as follows: white for loop 6 of the α-subunit, blue for the rest of α-subunit and red for the mobile region (residues 93−189) of the β-subunit, yellow for the rest of the β-subunit. Possible hydrogen bonds between two polar atoms are indicated with black dashed dots. (A) In the wild-type structure, βLys167 interacts with βAsp305, which is modeled as two alternative conformations (Table 5). The PLP internal aldimine is shown at the β active site. Residues αPro53−αPro78 and βSer161−βTyr181 form a part of α−β subunit interface and include helix α2′ in the α-subunit and helix α6 in the β-subunit, respectively. (B) In the βK87T-Ser-GP structure, there are more hydrogen bonds between the mobile region residues and the rest of the β-subunit (see text for details and Table 5). βLys167 and βArg175 in the mobile region interact with loop 2 residues in the α-subunit, and these interactions are observed in all four mutant complexes. Glycerol 3-phosphate and the external aldimine are shown at their binding sites at the α- and β-subunits.

and synthesis of IGP at the active site of the α-subunit are catalyzed by αGlu49 and αAsp60 (Kirschner et al., 1991; Nagata et al., 1989) (Figure 11).

The proposed role of αAsp60 is supported by the location of the carboxylate about 3.0 Å from the indole nitrogen of IPP (Figures 5A and 12). However, structural evidence for

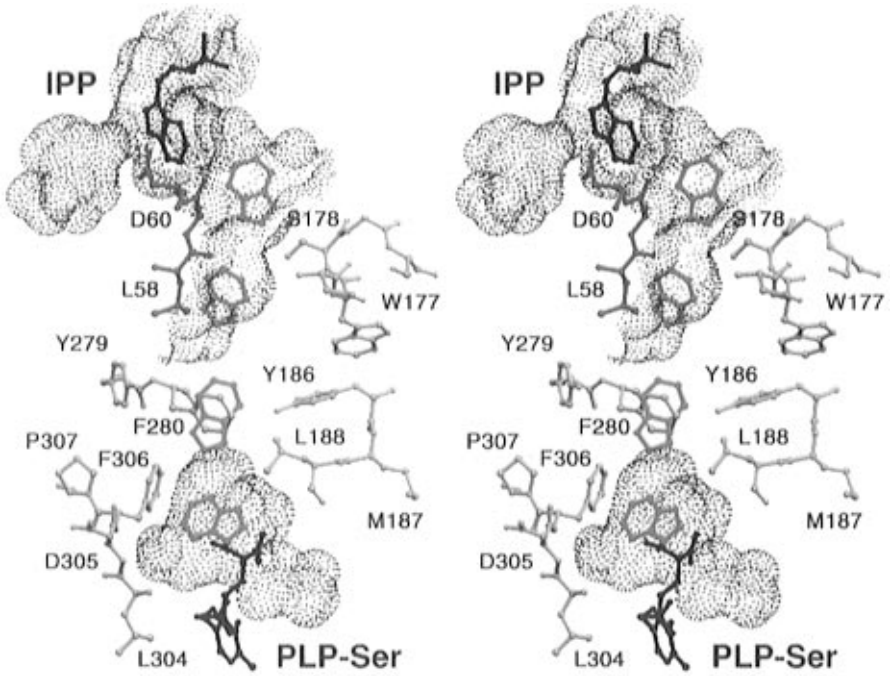

FIGURE 9: View of the indole tunnel between the α and β active sites of the βK87T-Ser-IPP $\alpha_2\beta_2$ complexes. Bound IPP and PLP-Ser are indicated in black, selected α-subunit residues in red, and β-subunit residues in lavender. Four indole molecules can be modeled inside of the tunnel (Hyde et al., 1988) and are represented in green, although there has been no direct observation of indole within the tunnel. Note that the side chain of βPhe280 is superimposed on the modeled indole at this location and the tunnel in this structure is blocked. The dot surface area is calculated using the program MS (Connolly, 1983) with a probe radius of 1.4 Å.

the proposed role of αGlu49 is less clear; the carboxylate is located approximately 6.1 Å from the modeled C3′ hydroxyl group in the IPP structure and about 4.8 Å in the GP structure. In the two structures the side chain of αGlu49 is not in an extended form but folds away from the location of the scissile bond (Figure 5). Because of the length and flexibility of the glutamate side chain it is possible that, with the true substrate IGP bound, the appropriate contact could be established. Further experiments to clarify this point are underway.

An important new feature of the active site of the α-subunit reported here is the closure of loop 6 in the βK87T-Ser-IPP and βK87T-Ser-GP structures (Figure 5 and Table 2). Loop 6 appears to function analogously to flexible loops in the same position in the 8-fold α/β barrel structures of triose-phosphate isomerase (Lolis & Petsko, 1990; Wierenga et al., 1991) and ribulose-1,5-bisphosphate carboxylase/oxygenase (Andersson et al., 1989; Curmi et al., 1992; Newman & Gutteridge, 1993) by moving from an open to a closed position in the presence of an active site ligand, effectively covering the active site. In the case of the α-subunit of tryptophan synthase, however, the open conformation is too disordered to be observed (Hyde et al., 1988).

In the closed conformation observed here, the hydroxyl group of αThr183 in loop 6 interacts with Oδ of αAsp60 in loop 2 and may play a role in positioning the carboxylate of αAsp60 for hydrogen bond formation with the indole nitrogen of IGP (see Figures 11 and 12). This structural feature would explain the role of αThr183, which is essential for catalysis (Yang & Miles, 1992) and which is one of the sites of missense mutations which inactivate the α-subunit in *Escherichia coli* (Yanofsky & Crawford, 1972).

Another residue in loop 6, αArg179, is involved in several hydrogen-bonding interactions with the neighboring loop 6 residues, αSer180, αVal182, and αGly184 (Figure 5A). Loss

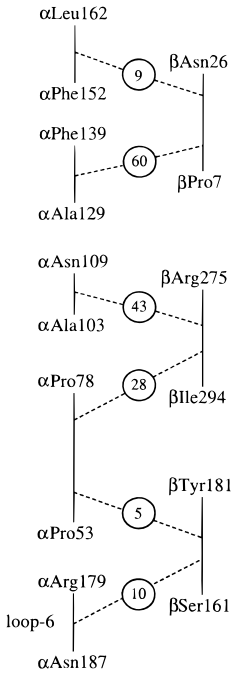

FIGURE 10: Schematic representation of the interface between the α- and β-subunits in the wild-type enzyme. Defined interface residues are α-subunit residues 53−62, 65, 69, 72, 77−78, 103−109, 129−135, 138−139, 152−157, 162, and 177 and β-subunit residues 7−8, 11, 14−23, 26, 161−162, 167−168, 171−172, 174−175, 181, 275−281, 283, 286, 288, and 290−294. These residues are located in four clusters in the α-subunit and in three clusters in the β-subunit (see Figure 6 for locations of these clusters relative to the structural elements in each subunit). The number of contacts, including polar and van der Waals interactions within 4.0 Å, between α−β interface residues in interacting clusters is indicated in circles. Loop 6 is also part of the interface residues in the βK87T-Ser-IPP and βK87T-Ser-GP structures and is included in this scheme.

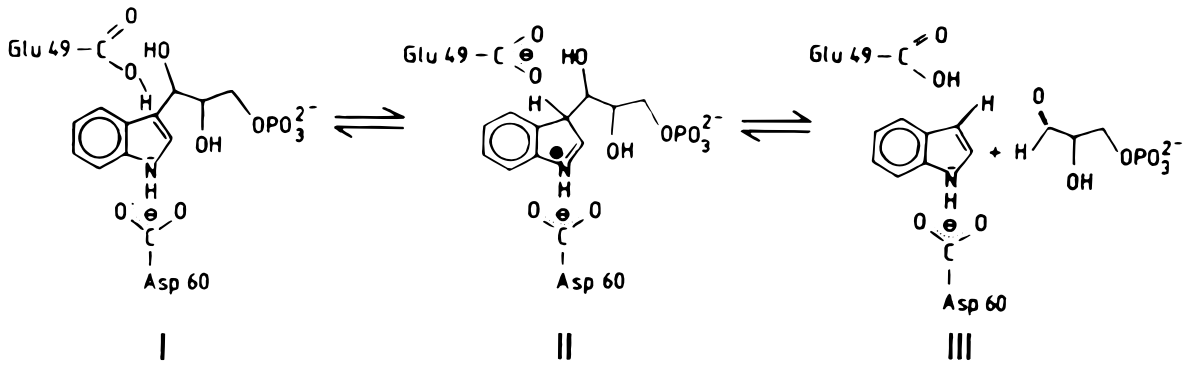

FIGURE 11: Proposed mechanism of the α reaction. The cleavage of indole-3-glycerol phosphate (I) is activated by tautomerization of the indole ring to yield the indolenine tautomer II which undergoes aldol cleavage to yield III. These steps are catalyzed by three putative residues, B_1, B_2, and B_3. The binding geometry of indole-3-propanol phosphate suggests that αAsp60 may serve as a B_2 residue which abstracts the proton on N-1 of the indole ring or forms a strong hydrogen bond to polarize the nitrogen atom. αGlu49 is thought to serve as a B_3, which accepts the proton on the hydroxyl group. αGlu49 may also serve as a B_1 that protonates the C3 position of the indole moiety. [Reproduced with permission from Miles et al. Copyright 1994 Kodansha, Ltd.]

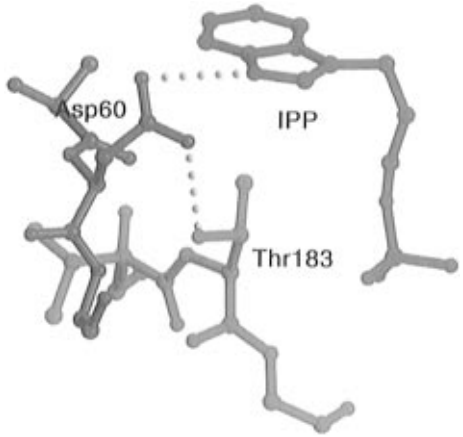

FIGURE 12: Hydrogen bond interactions in residues αThr183, αAsp60, and IPP. Possible interactions are represented by yellow dashed lines between the interacting atoms: 2.8 Å between αThr183 and αAsp60 and 3.2 Å between αAsp60 and IPP.

of these interactions upon mutation of αArg179 could explain why the αR179T mutation reduces the substrate binding affinity and affects the reciprocal communication between the α- and β-subunits (Brzović et al., 1993; Kawasaki et al., 1987).

We have considered the possible effect of loop 6 closure on the allosteric movements between the α- and β-subunits. Three residues in loop 6 (α180−182) make van der Waals interactions with the β-subunit and may influence the relative motions of the two subunits. More importantly, the ligand-induced interaction between αThr183 in loop 6 and αAsp60 in loop 2 (Figure 12) appears to stabilize loop 2 and may consequently stabilize the interaction of loop 2 residues 53−62 with residues in the β-subunit.

Relationships between the α-Subunit and Triosephosphate Isomerase. The tryptophan synthase α-subunit and triosephosphate isomerase (TIM) have a high level of structural homology and share a common substrate, D-glyceraldehyde 3-phosphate (Hyde et al., 1988). Crystallographic studies of TIM have shown that here too loop 6, which is four residues shorter than in tryptophan synthase, is flexible and moves nearly 7 Å from an open to a closed conformation upon binding of a transition-state analog, 3-phosphoglycolate (PGA), effectively covering the active site (Lolis & Petsko, 1990). Residues 179−191 in the α-subunit loop 6 appear to be highly disordered in the wild-type crystal structure both in the presence and in the absence of IPP (Hyde et al., 1988). The new results presented here indicate that the ordering of loop 6 requires the combined presence of ligands at both the active sites of the α- and β-subunits (i.e., in the βK87T-Ser-IPP and βK87T-Ser-GP structures).

A comparison of the closed structures of the α-subunit and TIM (Figure 13) shows an overall rms deviation of 3.03 Å for the Cα atoms. The major differences occurred in the α-helices and in the loops with good superposition of the eight β-strands. The phosphate groups of the IPP and PGA in the two structures are at almost identical positions (0.34 Å deviation for the phosphorus). The phosphate binding site is surrounded by two loops: one between β-strand 7 and helix 7 and the second between β-strand 8 and helix 8 for TIM or helix 8′ for tryptophan synthase. This phosphate binding site has also been shown to occur in the two preceding enzymes of the tryptophan biosynthesis pathway, phosphoribosyl anthranilate isomerase and indole glycerol phosphate synthase (Wilmanns et al., 1991).

In TIM and tryptophan synthase loop 6 performs similar structural and functional roles. Structurally, loop 6 interacts with the bound inhibitor mainly through van der Waals contacts, forming only one possible hydrogen bond with the phosphate oxygens of IPP or PGA. The nitrogens of αGly184 in tryptophan synthase and of Gly171 in TIM form hydrogen bonds with phosphate oxygens with lengths of 3.6 and 2.6 Å, respectively. Surface area calculations indicate that loop 6 buries the α active site of tryptophan synthase, as is also observed in TIM (Lolis & Petsko, 1990). Loop 6 may perform the same functional role in catalysis by closing the active site and isolating bound substrate from solvent.

Active Site and Catalytic Mechanism of the β-Subunit. The reaction of L-serine and indole catalyzed by the β-subunit proceeds through a series of PLP intermediates (Scheme 1A) (Davis & Metzler, 1972; Miles, 1986, 1991a). The crystal structure of the wild-type $\alpha_2\beta_2$ complex (Hyde et al., 1988) located the binding site of the PLP coenzyme but not the binding site of the substrate or product. PLP is bound to the wild-type β-subunit as an internal aldimine with βLys87 (E in Scheme 1A). The external aldimines E-Ser and E-Trp formed by the mutant βK87T $\alpha_2\beta_2$ complex (Scheme 1B) serve as models for the corresponding intermediates formed by the wild-type enzyme. However, the possibility remains that the mutant enzyme may differ in some ways from the wild-type enzyme. Surprisingly, the replacement of the

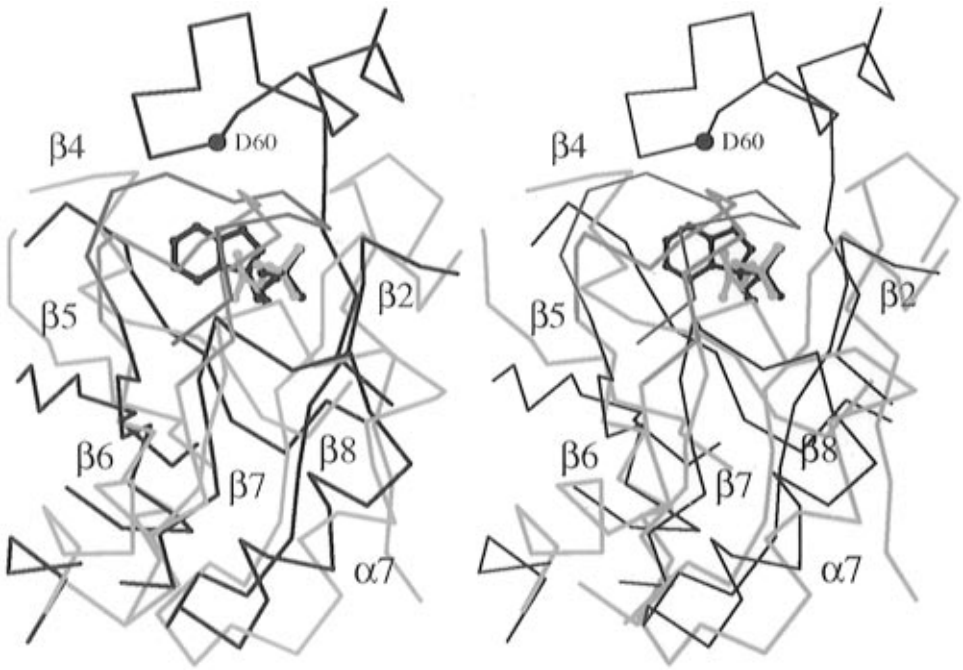

FIGURE 13: Comparison of the substrate binding sites and loop 6 in the α-subunit of tryptophan synthase (TS; black) and in TIM (sky blue; 2ypi in PDB entry name with residues 2−248). Loop 6 is indicated with red for TS and green for TIM. For clarity, β-strands 1 and 3 are not included in this drawing though those strands are also aligned well. Residues 190−193 of the α-subunit of TS are highly disordered and thus are not modeled. Major differences near the active site between the two structures are the presence of extra residues for loop 2 and helix 2′ in the α-subunit of TS. Catalytic residue αAsp60 in loop 2 of TS is indicated by the filled circle at its Cα position. The two structures have been compared using the program ALIGN [Cohen in Satow et al. (1986)].

lysine side chain by threonine does not appear to result in the addition of more bound water molecules in the vicinity of the missing side chain atoms. Also, the PLP is located in much the same position that it occupies in the internal aldimine of the wild-type enzyme. These observations support the view that this βK87T mutant structure is truly representative of the reaction intermediate.

The role of PLP is to act as an electron sink to stabilize the carbanionic intermediates that develop during enzymatic catalysis between E-Ser and E-AA in Scheme 1A (Walsh, 1979). The first step in the β-subunit-catalyzed reaction with L-serine is removal of the α-proton to yield a carbanionic intermediate. In the case of aspartate aminotransferase, this step is facilitated by electron withdrawal from Cα to the positively charged pyridinium nitrogen N1 of PLP. Aspartate aminotransferase stabilizes the carbanionic intermediate by an ionic interaction between the side chain carboxylate of Asp222 and N1 of PLP (Jansonius & Vincent, 1987; Rhee, 1994). However, there are no such acidic residues in the β-subunit close to N1 of PLP that could serve this role. The hydroxyl group of βSer377 may form a hydrogen bond with the unprotonated N1 of PLP which is about 3.0 Å distant. The carboxylate of βGlu350 is too distant (more than 4 Å) from the coenzyme ring and is in the wrong orientation to interact with N1.

In the external aldimine of βK87T-Trp (Scheme 1), βGlu109 makes the only polar interaction with the indole side chain and forms a strong hydrogen bond with the indole nitrogen (Figure 2f). It has been postulated that the carboxylate of βGlu109 is important in activating the indole toward nucleophilic attack on the aminoacrylate intermediate (E-AA) (Kayastha & Miles, 1990; Miles et al., 1991). This hypothesis is supported by kinetic studies with a mutant enzyme having βGlu109 replaced by aspartate (Anderson et al., 1991; Brzović et al., 1992a). However, βGlu109 is clearly not an essential residue for catalysis since a mutant enzyme with βGlu109 replaced by alanine has considerable activity in the conversion of β-chloro-L-alanine and indole to L-tryptophan (Ahmed et al., 1991).

Investigations of the stereochemistry of reactions catalyzed by tryptophan synthase have demonstrated that enzyme-mediated group transfers occur on only one face of the coenzyme−substrate complex, the *si* face (Dunathan & Voet; 1974; Miles et al., 1982; Schleicher et al., 1976; Skye et al., 1974; Tsai et al., 1978). The external aldimines in the βK87T-Ser and βK87T-Trp structures are largely planar and the scissile Cα−H bond is located on the *si* face of the plane. The side chain of βLys87 in the wild-type structure is also located on the *si* face of the plane and is in a favorable position to abstract the α-proton from the external aldimines of both L-serine and L-tryptophan. Thus, the observed results support the mechanism shown in Scheme 1A, in which βLys87 first deprotonates E-Ser and later protonates E-Q to form E-Trp on the same face of the plane, retaining the stereochemistry of the L-amino acid. The location of the scissile Cα−H bond is perpendicular to the plane of the π-bonding system of the coenzyme. The delocalized π-electrons from the pyridine ring to the amino group of the external aldimine stabilize the quinonoid intermediate after the deprotonation step, in accordance with Dunathan's proposal (Dunathan, 1971).

Conformational Changes in the α- and β-Subunits Induced by Bound Ligands. A number of kinetic and spectroscopic investigations have provided evidence for ligand-mediated reciprocal communication between the α- and β-subunits. These allosteric interactions are thought to regulate transitions between conformationally open and closed states of the protein (Brzović et al., 1992b,c, 1993; Dunn et al., 1994; Houben & Dunn, 1990; Kirschner et al., 1991; Pan & Dunn, 1996; Ruvinov et al., 1995a,b). In this study, we have

observed different conformational states of both subunits on binding of ligands, which can be related to the allosteric movements between the α- and β-subunits.

Comparison of the βK87T-Ser and the wild-type structures shows virtually no differences in the α-subunit but small differences in β-subunit (Figure 6). These differences may result from interactions between the carboxylate of the serine moiety and residues 110−115 in the N-terminal domain of the β-subunit (Figure 2). Comparison of the βK87T-Trp structure with the wild-type structure shows much larger conformational changes in both α- and β-subunits. These are similar to the changes observed in the βK87T-Ser-IPP and βK87T-Ser-GP structures, with the exception of the α-subunit loop 6, which remains highly disordered and cannot be modeled. The observed changes include a rotation of the α-subunit and the movement of the mobile region which includes the movement of βGlu109 to a position near the indolyl nitrogen of L-tryptophan (Figure 2).

Comparison of the IPP and GP complexed structures with the uncomplexed βK87T-Ser structure shows that the binding of IPP or GP in the α-subunit produces conformational changes in both the α-subunit and in the distant β-subunit. The α-subunit rotates relative to the β-subunit by approximately 5°. It is noteworthy that binding of tryptophan to the active site of the β-subunit in the βK87T-Trp structure results in similar changes in the distant α-subunit, including the 5° rotation. These structural changes must be transmitted through the α−β subunit interface which includes interactions between residues in the α-subunit loop 2 (residues 53−62) and residues in the N-terminal domain (residues 161−181) of the β-subunit. These interface residues undergo significant conformational changes in these complex structures but leave the interactions between the subunits largely unchanged because the interface residues carry out concerted movements in the same direction.

In contrast, the interactions of the interdomain residues within the β-subunit are more strongly affected by the conformational changes in the mutant structures (Table 5 and Figure 8). Notable changes include the movements of β-subunit residues Arg141, Gln142, and Arg148 closer to residues Asp305, Lys382, Asp383, and Thr386. Investigations of a mutant $\alpha_2\beta_2$ complex having βAsp305 replaced by asparagine (D305N) attributed alterations in reaction and substrate specificity to the inability of the enzyme to undergo conversion from an "open" to a "closed" form (Ahmed et al., 1991). Similar results are also observed from enzymes with mutations at position βLys382 or βAsp383, which retain very low activity with L-serine, less than 1% of the wild-type enzyme (Yang et al., 1997). Our structural results suggest that the interactions of these interdomain residues may be essential for allosteric regulations including the conformational changes of the enzyme that have been seen in the IPP and GP complexed structures.

CONCLUSIONS

The results presented here provide a structural basis for increased understanding of the catalytic mechanism of the α- and β-subunits of tryptophan synthase and of ligand-dependent reciprocal communication between the α- and β-subunits. Our most important results are the identification of residues in the substrate binding site of the β-subunit, the demonstration of the ligand-induced closure of loop 6 over the active site of the α-subunit, and detection of other ligand-dependent conformational changes in the α- and β-subunits. These ligand-induced conformational changes demonstrate the structural effects of allosteric interactions that contribute to the control and coordination of the catalytic steps in the biosynthesis of L-tryptophan. The results provide a basis for the design of further experiments to correlate the structural and functional properties of tryptophan synthase.

ACKNOWLEDGMENT

We thank Dr. Joseph Ferrara, Molecular Structure Corp., for help with data collection for the βK87T-Trp complex.

REFERENCES

Ahmed, S. A., Miles, E. W., & Davies, D. R. (1985) *J. Biol. Chem. 260*, 3716−3718.
Ahmed, S. A., Ruvinov, S. B., Kayastha, A. M., & Miles, E. W. (1991) *J. Biol. Chem. 266*, 21540−21557.
Anderson, K. S., Miles, E. W., & Johnson, K. A. (1991) *J. Biol. Chem. 266*, 8020−8033.
Andersson, I., Knight, S., Schneider, G., Lindqvist, Y., Lundqvist, T., Branden, C.-I., & Lorimer, G. H. (1989) *Nature 337*, 229−234.
Banik, U., Zhu, D.-M., Chock, P. B., & Miles, E. W. (1995) *Biochemistry 34*, 12704−12711.
Brünger, A. T. (1992) *X-PLOR Version 3.1. A system for X-ray crystallography and NMR*, Yale University Press, New Haven, CT.
Brzović, P. S., Kayastha, A. M., Miles, E. W., & Dunn, M. F. (1992a) *Biochemistry 31*, 1180−1190.
Brzović, P. S., Ngo, K., & Dunn, M. F. (1992b) *Biochemistry 31*, 3831−3839.
Brzović, P. S., Sawa, Y., Hyde, C. C., Miles, E. W., & Dunn, M. F. (1992c) *J. Biol. Chem. 267*, 13028−13038.
Brzović, P. S., Hyde, C. C., Miles, E. W., & Dunn, M. F. (1993) *Biochemistry 32*, 10404−10413.
Carson, M. (1987) *J. Mol. Graphics 5*, 103−106.
Cohen, H. G. (1986) *J. Appl. Crystallogr. 19*, 486−488.
Connolly, M. L. (1983) *J. Appl. Crystallogr. 16*, 548−558.
Crawford, I. P. (1960) *Biochim. Biophys. Acta 45*, 405−407.
Curmi, P. M. G., Cascio, D., Sweet, R. M., Eisenberg, D., & Schreuder, H. (1992) *J. Biol. Chem. 267*, 16980−16989.
Davis, L., & Metzler, D. E. (1972) in *The Enzymes* (Boyer, P. D., Ed.) Vol. 7, pp 33−74, Academic Press, New York.
Dunathan, H. C. (1971) *Adv. Enzymol. 35*, 79−134.
Dunathan, H. C., & Voet, J. G. (1974) *Proc. Natl. Acad. Sci. U.S.A. 71*, 3888−3891.
Dunn, M. F., Brzović, P. S., Leja, C., Pan, P., & Woehl, E. U. (1994) in *Biochemistry of Vitamin B6 and PQQ* (Marino, G., Sannia, G., & Bossa, F., Eds.) pp 119−124, Birkhauser Verlag, Basel, Switzerland.
Gerstein, M., & Chothia, C. (1991) *J. Mol. Biol. 220*, 133−149.
Hendrickson, W. A. (1985) *Methods Enzymol. 115*, 252−270.
Hendrickson, W. A., & Konnert, J. H. (1981) in *Biomolecular Structure, Conformation, Function, and Evolution* (Srinivasan, R., Ed.) pp 43−57, Pergamon, Oxford.
Houben, K. F., & Dunn, M. F. (1990) *Biochemistry 29*, 2421−2429.
Hyde, C. C., Ahmed, S. A., Padlan, E. A., Miles, E. W., & Davies, D. R. (1988) *J. Biol. Chem. 263*, 17857−17871.
Jansonius, J. N., & Vincent, M. G. (1987) in *Biological Macromolecules & Assemblies* (Jurnak, F. A., & McPherson, A., Eds.) pp 187−288, Wiley & Sons, New York.
Jones, T. A., Zou, J. Y., Cowan, S. W., & Kjeldgaard, M. (1991) *Acta Crystallogr. A47*, 110−119.
Kawasaki, H., Bauerle, R., Zon, G., Ahmed, S. A., & Miles, E. W. (1987) *J. Biol. Chem. 262*, 10678−10683.
Kayastha, A. M., & Miles, E. W. (1990) *FASEB J. 4*, A2118.
Kirschner, K., Lane, A. N., & Strasser, A. W. M. (1991) *Biochemistry 30*, 472−478.
Lesk, A. M. (1991) *Protein Architecture: a Practical Guide*, IRL Press, Oxford.

Lolis, E., & Petsko, G. (1990) *Biochemistry 29*, 6619−6625.
Lu, Z., Nagata, S., Mc Phie, P., & Miles, E. W. (1993) *J. Biol. Chem. 268*, 8727−8734.
Metzler, D. E., Ikawa, M., & Snell, E. E. (1954) *J. Am. Chem. Soc. 76*, 648−652.
Miles, E. W. (1979) *Adv. Enzymol. 49*, 127−186.
Miles, E. W. (1986) in *Pyridoxal Phosphate and Derivatives* (Dolphin, D., Poulson, D., & Avramovic, O., Eds.) pp 253−310, John Wiley and Sons, New York.
Miles, E. W. (1991a) *Adv. Enzymol. Relat. Areas Mol. Biol. 64*, 93−172.
Miles, E. W. (1991b) *J. Biol. Chem. 266*, 10715−10718.
Miles, E. W. (1995) in *Subcellular Biochemistry, Vol 24: Proteins: Structure, Function, and Protein Engineering* (Biswas, B. B., & Roy, S., Eds.) pp 207−254, Plenum Press, New York.
Miles, E. W., Houck, D. R., & Floss, H. G. (1982) *J. Biol. Chem. 257*, 14203−14210.
Miles, E. W., Kawasaki, H., Ahmed, S. A., Morita, H., Morita, H., & Nagata, S. (1989) *J. Biol. Chem. 264*, 6280−6287.
Miles, E. W., Ahmed, S. A., & Kayastha, A. M. (1991) Enzymes dependent on pyridoxal phosphate and other carbonyl compounds as cofactors, in *Proceedings of the 8th International Symposium on Vitamin B6 and Carbonyl Catalysis* (Fukui, T., Kagamiyama, H., Soda, K., & Wada, H., Eds.) pp 249−256, Pergamon Press, New York.
Miles, E. W., Ahmed, S. A., Hyde, C. C., Kayastha, A. M., Yang, X.-J., Ruvinov, S. B., & Lu, Z. (1994) in *Molecular Aspects of Enzyme Catalysis* (Fukui, T., & Soda, K., Eds.) pp 127−146, Kodansha, Ltd., Tokyo, Japan.
Nagata, S., Hyde, C. C., & Miles, E. W. (1989) *J. Biol. Chem. 264*, 6288−6296.
Newman, J., & Gutteridge, S. (1993) *J. Biol. Chem. 268*, 25876−25886.
Pan, P., & Dunn, M. F. (1996) *Biochemistry 35*, 5002−5013.
Peracchi, A., Mozzarelli, A., & Rossi, G. L. (1995) *Biochemistry 34*, 9459−9465.
Perutz, M. F. (1989) *Mechanism of cooperativity and allosteric regulation in proteins*, Cambridge University Press, Cambridge.
Rhee, S. (1994) Ph.D. Thesis, The University of Iowa, Iowa City, IA.
Rhee, S., Parris, K., Ahmed, S. A., Miles, E. W., & Davies, D. R. (1996) *Biochemistry 35*, 4211−4221.
Ruvinov, S. B., & Miles, E. W. (1992) *FEBS Lett. 299*, 197−200.
Ruvinov, S. B., Ahmed, S. A., McPhie, P., & Miles, E. W. (1995a) *J. Biol. Chem. 270*, 17333−17338.
Ruvinov, S. B., Yang, X.-J., Parris, K., Banik, U., Ahmed, S. A., Miles, E. W., & Sackett, D. L. (1995b) *J. Biol. Chem. 270*, 6357−6369.
Satow, Y, Cohen, G. H., Padlan, E. A., & Davies, D. R. (1986) *J. Mol. Biol. 190*, 593−604.
Schleicher, E., Mascaro, K., Potts, R., Mann, D. R., & Floss, H. B. (1976) *J. Am. Chem. Soc. 98*, 1043−1044.
Sheriff, S. (1987) *J. Appl. Crystallogr. 20*, 55−57.
Shirvanee, L., Horn, V., & Yanofsky, C. (1990) *J. Biol. Chem. 265*, 6624−6625.
Skye, G. E., Potts, R., & Floss, H. G. (1974) *J. Am. Chem. Soc. 96*, 1593−1595.
Swift, S., & Stewart, G. S. (1991) *Biotechnol. Genet. Eng. Rev. 9*, 229−294.
Tsai, M. D., Schleicher, E., Potts, R., Skye, G. E., & Floss, H. G. (1978) *J. Biol. Chem. 253*, 5344−5349.
Walsh, C. T. (1979) *Enzymatic Reaction Mechanisms*, pp 775−827, Freeman and Co., New York.
Wierenga, R. K., Noble, M. E. M., Postma, J. P. M., Groendijk, H., Kalk, K. H., Hol, W. G. J., & Opperdoes, F. R. (1991) *Proteins 10*, 33−49.
Wilmanns, M., Hyde, C. C., Davies, D. R., Kirschner, K., & Jansonius, J. N. (1991) *Biochemistry 30*, 9161−9169.
Woehl, E. U., & Dunn, M. F. (1995) *Biochemistry 34*, 9466−9476.
Yang, L.-h., Ahmed, S. A., Rhee, S., & Miles, E. W. (1997) *J. Biol. Chem. 272*, 7859−7866.
Yang, X.-J., & Miles, E. W. (1992) *J. Biol. Chem. 267*, 7520−7528.
Yanofsky, C., & Crawford, I. P. (1972) in *The Enzymes* (Boyer, P. D., Ed.) pp 1−31, Academic Press, New York.
Yutani, K., Ogasahara, K., Tsujita, T., Kanemoto, K., Matsumoto, M., Tanaka, S., Miyashita, T., Matsushiro, A., Sugino, Y., & Miles, E. W. (1987) *J. Biol. Chem. 262*, 13429−13433.

BI9700429